



Lake dwellers occupation gap in Lake Geneva (France–Switzerland) possibly explained by an earthquake–mass movement–tsunami event during Early Bronze Age



Katrina Kremer^{a,b,*}, François Marillier^c, Michael Hilbe^{d,e}, Guy Simpson^a, David Dupuy^c, Ble J.F. Yrro^{c,1}, Anne-Marie Rachoud-Schneider^f, Pierre Corboud^g, Benjamin Bellwald^e, Walter Wildi^h, Stéphanie Girardclos^{a,b}

^a Department of Earth Sciences, University of Geneva, Rue des Maraîchers 13, 1205 Geneva, Switzerland

^b Institute for Environmental Sciences, University of Geneva, Site de Batelle, Carouge, Switzerland

^c Research Centre in Terrestrial Environment, University of Lausanne, Geopolis Bldg., 1015 Lausanne, Switzerland

^d Eawag, Swiss Federal Institute of Aquatic Science and Technology, Ueberlandstrasse 133, 8600 Dübendorf, Switzerland

^e Institute of Geological Sciences, University of Bern, Baltzerstrasse 1+3, 3012 Berne, Switzerland

^f Musée et Jardins botaniques cantonaux, Avenue de Cour 14bis, 1007 Lausanne, Switzerland

^g Archéologie préhistorique et anthropologie, Institute Forel, University of Geneva, Route des Acacias 18, 1211 Geneva, Switzerland

^h Institute F.-A. Forel, University of Geneva, Route de Suisse 10, 1290 Versoix, Switzerland

ARTICLE INFO

Article history:

Received 8 May 2013

Received in revised form 10 September 2013

Accepted 12 September 2013

Available online 6 November 2013

Editor: P. Shearer

Keywords:

lake dwellers
Lake Geneva
mass movement
earthquake
tsunami

ABSTRACT

High-resolution seismic and sediment core data from the ‘Grand Lac’ basin of Lake Geneva reveal traces of repeated slope instabilities with one main slide-evolved mass-flow (minimum volume 0.13 km³) that originated from the northern lateral slope of the lake near the city of Lausanne. Radiocarbon dating of organic remains sampled from the top of the main deposit gives an age interval of 1865–1608 BC. This date coincides with the age interval for a mass movement event described in the ‘Petit Lac’ basin of Lake Geneva (1872–1622 BC). Because multiple mass movements took place at the same time in different parts of the lake, we consider the most likely trigger mechanism to be a strong earthquake (Mw 6) that occurred in the period between 1872 and 1608 BC. Based on numerical simulations, we show the major deposit near Lausanne would have generated a tsunami with local wave heights of up to 6 m. The combined effects of the earthquake and the following tsunami provide a possible explanation for a gap in lake dwellers occupation along the shores of Lake Geneva revealed by dendrochronological dating of two palafitte archaeological sites.

© 2013 The Authors. Published by Elsevier B.V. Open access under [CC BY-NC-ND license](#).

1. Introduction

In the Neolithic and Bronze age, raised stilt house (or palafitte or lake dwelling) settlements were common around peri-Alpine lakes. Since 2011, a representative selection of 111 prehistoric lake dwellings has been inscribed on UNESCO’s World Heritage list in six countries bordering the Alps: France, Germany, Austria, Italy, Slovenia and Switzerland (<http://whc.unesco.org/en/list/1363/>). Such house remains, present on the shores of Lake Geneva as underwater fields of wooden piles, can be accurately dated with dendrochronology to obtain the exact year of tree cutting. The occurrence of continuous series of dated piles defines the (minimum)

* Corresponding author at: Department of Earth Sciences, University of Geneva, Rue des Maraîchers 13, 1205 Geneva, Switzerland. Tel.: +41 22 379 31 64.

E-mail address: katrina.kremer@unige.ch (K. Kremer).

¹ Present address: Département des génies civil, géologique et des mines, Polytechnique Montreal, C.P. 6079, Montréal, Quebec, Canada.

lake dweller occupation interval of lake shores. In Lake Geneva, pile data show a 21 years-long period of continuous tree cutting and house building at Preverenges, ending in 1758 BC, followed by the building of new pile houses starting in 1730 BC, 3 km away in Morges/Les Roseaux (Fig. 1; Corboud and Pugin, 2008). However in Preverenges, new pile houses building started only 129 years later in 1625 BC. This 28 years interval without dated piles is interpreted as a human occupation gap. Such human occupation gaps are generally explained by an increase in lake-level, soil depletion or social and cultural changes (Magny, 2004; Corboud, 2012; Magny et al., 2012; Swierczynski et al., 2013).

For several of the peri-Alpine lakes occupied by palafitte settlements, large-scale subaqueous mass movement events, transporting large amounts of sediment from lateral slopes to the deep basins, have been reconstructed based on sedimentological and geophysical evidence (Chapron et al., 1999; Arnaud et al., 2002; Schnellmann et al., 2006; Strasser and Anselmetti, 2008; Smith et al., 2013; Strasser et al., 2013; Wilhelm et al., 2013). These mass

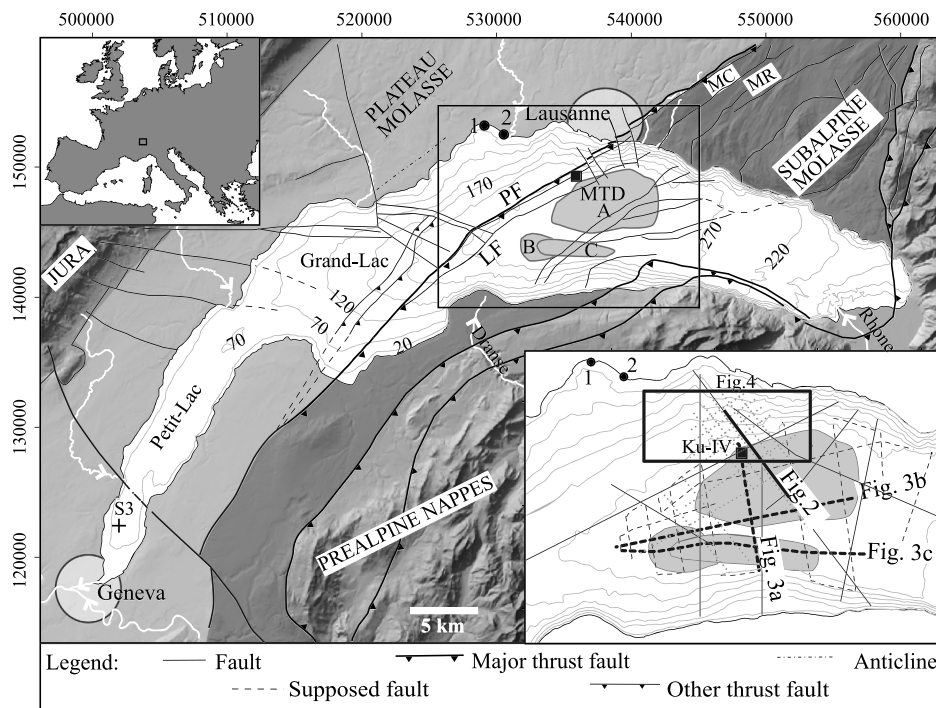


Fig. 1. Shaded digital elevation model (Swiss Federal Office of Topography) of the region surrounding Lake Geneva with the main rivers, cities as well as tectonic units and faults (in black) after the Swiss tectonic map (1:500 000) and Dupuy (2006). PF: Paudeze Fault; LF: Lutrive Fault; MC: Molasse à charbon; MR: Molasse rouge. General bathymetry (m) is given by grey contour lines. The areal extent of mass transport deposits within the lake sediments (MTDs A, B, and C; this study) is indicated in grey. Black dots refer to archaeological palafitte sites (1: Morges VD–Les Roseaux, 2: Preverenges, after Corboud and Pugin, 2008). Black square (Ku-IV) and cross (S3) locate sediment core and drilling, respectively. The inset map locates seismic reflection airgun (black), watergun (dotted) and pinger (dashed) lines with references to profiles of Figs. 2 and 3 (bold lines) and multibeam bathymetry data (black rectangle) with reference to Fig. 4. Coordinates are in meters (Swiss Grid).

movements have the potential to produce tsunamis with heights reaching several metres, which constitute a considerable natural hazard along the shores of these lakes (Kremer et al., 2012). A common trigger mechanism for slope instabilities in this environment is earthquake shaking, which often leads to widespread mass transport, producing coeval deposits in different parts of a lake or even in more than one lake (Schnellmann et al., 2002; Strasser et al., 2006, 2013). Current research shows that initial sublacustrine mass movements (slides, slumps...) often produce complex mass transport deposits (Mulder and Cochonat, 1996; Schnellmann et al., 2006 and references therein) including mass wasting and mass-flow deposits in the same bed.

Here, we propose an alternative explanation for the observed occupation gap of the palafitte settlements on Lake Geneva, involving the combined effects of a large earthquake that triggered mass movements and a tsunami in the lake. As evidence, we present new seismic reflection, sedimentological, palynological data and new ^{14}C dates along with results of tsunami wave numerical modelling.

2. Geological setting

Lake Geneva is the largest freshwater basin in Western Europe with a water volume of 89 km^3 extending over an area of 580.1 km^2 . It is divided into two sub-basins; the 'Grand Lac', the lake's main part with a maximum water depth of 309 m and the 'Petit Lac' at its western end with a maximum water depth of 70 m (Fig. 1). Lake Geneva is situated in the Alpine foreland between the Alps and the Jura mountain ranges and was carved during Quaternary glaciations mostly into the Tertiary Molasse.

The Molasse bedrock comprises two tectonic units: the relatively undeformed, south-east dipping Plateau Molasse and a complex assemblage of imbricated thrust slices, the Subalpine Molasse (Gorin et al., 1993; Sommaruga et al., 2012). In the region of

Lake Geneva, these two units are divided by the 'Paudeze Fault' (PF) zone (Fig. 1), which is a major thrust fault with a vertical throw of 1 km in the vicinity of the city of Lausanne and a southwest–northeast trend (Weidmann, 1998). This fault zone runs through the city of Lausanne, across the lake and reappears on the southern shore (Dupuy, 2006; Scheidhauer et al., 2005; Weidmann, 1998). Towards the east, a second fault system, called 'Lutrive Fault' (LF), separates two subunits of the Subalpine Molasse: the 'Molasse à charbon' (MC) and the 'Molasse rouge' (MR).

Quaternary sediments in Lake Geneva have a maximum thickness of 400 m (Dupuy, 2006; Vernet et al., 1974). They consist mainly of moraines, pro- and peri-glacial units and lacustrine deposits. The geometry of the lacustrine infill is complex and varies greatly depending on its location and age (Girardclos et al., 2005; Loizeau, 1991). In areas exposed to deep current erosion (Girardclos et al., 2003), such as the junction between the two sub-basins and the Versoix area, Holocene lacustrine sediment thickness is close to zero, whereas in the Rhone delta area it reaches 400 m (Dupuy, 2006). Holocene background hemipelagic sediments are often 5–10 m thick but mixing and deposition together with clastic sediments, brought by lateral rivers such as Dranse, Aubonne, Versoix, Promenthouse, and Venoge, generally increase lacustrine sediment thickness to 20–75 m near deltas (Baster et al., 2003; Dupuy, 2006; Fiore, 2007; Fiore et al., 2011). Analogously, the sediment accumulation rate for the past 50 years varies between 0.01 and $1.96 \text{ g cm}^{-2} \text{ yr}^{-1}$, thus reflecting the locally highly variable sediment input (Corella et al., in press; Loizeau et al., 2012).

From historical and instrumental data, six earthquakes with $M_w > 4.5$ occurred in the Prealps, south east of the lake, in the period between 1500 and 2009 in Lake Geneva region (Table A1, Fig. A1; Fäh et al., 2011). In the same period, the area north of Lake Geneva was seismically less active, with only low-magnitude

Table 1
Radiocarbon ages from organic macro-remains (leaves and wood). Calibration was performed with the 'calibrate' function of the 'clam' code (Blaauw, 2010) for the open-source statistical software 'R', using the northern hemisphere terrestrial IntCal09 calibration data (Reimer et al., 2009).

Sediment core	Sediment core depth (cm)	Lab No.	Conventional radiocarbon age (^{14}C yr BP)	2σ calibration (cal. yr BP)	2σ calibration (BC/AD)	Probability (%)	Dated material
Ku-IV	656.5	ETH-47291	1857 \pm 41	1707 to 1882	68 to 243	95	Leaves
Ku-IV	750	ETH-42345	2255 \pm 40	2154 to 2272 2293 to 2345	–322 to –204 –395 to –343	62.4 32.5	Leaves
Ku-IV	807	ETH-47920	2648 \pm 55	2549 to 2557 2617 to 2634 2704 to 2877 2914 to 2916	–607 to –599 –684 to –667 –927 to –754 –966 to –964	0.5 1.7 92.6 0.1	Leaves
Ku-IV	929	ETH-43010	3395 \pm 35	3558 to 3723 3797 to 3815	–1773 to –1608 –1865 to –1847	93.2 1.8	Leaves
S3	680	ETH-40226	3415 \pm 35	3572 to 3727 3749 to 3764 3793 to 3822	–1777 to –1622 –1814 to –1799 –1872 to –1843	86.4 2.2 6.4	Wood

earthquakes (Mw 2–4) occurring mostly near fault zones of the Molasse units (Fig. A1; Deichmann et al., 2012; Fäh et al., 2011).

3. Methods

3.1. Seismic and multibeam data

We have conducted several seismic and coring campaigns on Lake Geneva (Fig. 1). Since 2000, a large number of multi-channel reflection profiles were acquired as part of several Master and PhD theses at the University of Lausanne; a few of them were used for the present work. The profiles were acquired with a S15 Soderia watergun or with a Soderia Mini GI airgun, GPS navigation (positioning error 3–5 m) or DGPS (positioning error \pm 20 cm) and recorded with either a Bison or a Geometrics seismograph.

The airgun data have a dominant frequency of 330 Hz and a theoretical vertical resolution of 1.1 m at 1500 m/s, whereas the watergun data have a dominant frequency of 670 Hz and theoretical vertical resolution of 0.56 m. The streamer was composed of two to three interconnected solid-state streamers with either 48 or 64 hydrophones spaced at 2.5 m intervals and one hydrophone per channel. The minimum offset was 5 m and the maximum offset was 122.5 m and 162.5 m for the 48 and 64 hydrophones settings, respectively. The guns were fired at 5 or 10 m intervals providing a nominal fold of 6 to 16. The data were processed either with the Geovecteur software (CGG) or with visual-SUNT (Geo2x, a Windows adaptation of the SEISMIC UNIX modules). Processing included the following steps: geometry assignment, trigger-delay correction, first-arrival muting, trace editing, spherical divergence correction, predictive deconvolution, bandpass filtering, stacking and migration.

In April 2010, single-channel seismic reflection profiles were acquired with a 3.5 kHz pinger system and GPS navigation (positioning error of 3–5 m). These seismic data with a theoretical vertical resolution of 0.1 m were processed with SPW software, performing only bandpass filtering (2300–6500 Hz).

Seismic interpretation of the airgun, watergun and pinger data was conducted with the SMT Kingdom Suite software. Airgun data typically reach 300 to 400 ms two-way travel time (TWT) below the lake bottom, corresponding to 225 to 300 m using a 1500 m/s velocity for sediments. Penetration depth of the watergun data is up to 250 ms TWT, corresponding to \sim 180 m sediment depth. Pinger data reach a penetration of up to 50 ms TWT, corresponding to a sediment depth of \sim 40 m. The volumes of the mass transport deposits (MTD) were calculated using SMT Kingdom Suite, Supplementary Appendix B (Supplementary Methods).

High-resolution multibeam bathymetry data of the northern lateral slope off Lausanne (Fig. 1) are available from a bathymet-

ric mapping programme of Lake Geneva carried out in 2013 and funded by public agencies including the state of Vaud (Direction générale de l'environnement). This survey was performed using a Kongsberg EM2040 multibeam echosounder, operated at 300 kHz and providing 400 equidistant beams with $1^\circ \times 1^\circ$ beam width over a variable swath angle of \sim 80° to 150°. RTK-GPS positioning and a Kongsberg Seatex MRU5+ motion sensor directly attached to the transducers were used as auxiliary sensors. For analysis, a gridded data set with 2 m cell size was produced.

3.2. Sediment analysis

Based on the analysis of the seismic reflection data, a 12 m-long sediment core (Ku-IV; Fig. 1) was retrieved from the 'Grand Lac' basin at 300 m water depth with a modified Kullenberg-type gravity piston coring system (Kelts et al., 1986). Before opening, the core was scanned with a Geotek multisensor core logger (bulk density, magnetic susceptibility, sonic velocity) at 5 mm resolution. The core was then split in halves, photographed and sedimentologically described.

In the 'Petit Lac', a 70 m-long core S3 (Fig. 1) was drilled at a water depth of 40 m for a bridge/tunnel project in May 2009 with a geotechnical rotary system. This core was stored in wooden boxes, in which it was sedimentologically described, photographed and sampled.

3.3. Dating and palynology

The age model of sediment core Ku-IV is based on four AMS ^{14}C dates (Table 1) from terrestrial leaf remains and on the inferred age of a large turbidite deposited during the Tauredunum event in AD 563 (Kremer et al., 2012). Calibration was performed with the 'calibrate' function of the 'clam' code (Blaauw, 2010) for the open-source statistical software 'R', using the northern hemisphere terrestrial IntCal09 calibration data (Reimer et al., 2009). The age model was linearly interpolated between inferred ages using the 'clam' script. Ages are given with 95% confidence interval. Dates are given in years BC in order to compare with archaeological dates.

For sediment core S3 (0–43.35 m sediment depth), one AMS radiocarbon date from a wood fragment is available (Table 1). Additionally, pollen counting was carried out on S3. Samples were prepared as follows: HCl, whirlmixing in SPT, flotation in SPT, acetolysis, KOH, glycerin and staining with fuchsin. Lycopodium tablets were added to the samples (30 to 60 g) in order to estimate concentrations and influx. The subdivision of pollen diagrams into biozones and the chronology were established by comparison with local (Lotter, 1999; Moscarriello et al., 1998; Reynaud, 1982)

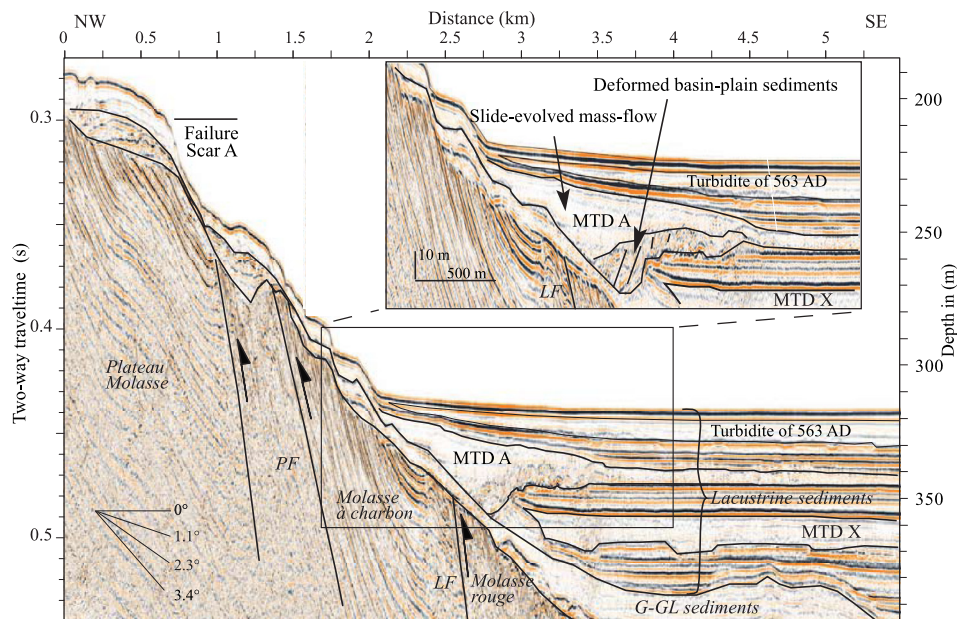


Fig. 2. Airgun seismic reflection section through the area of MTD A, showing the failure scar escarpment A and the acoustic signature of deep sedimentary infill interpreted as lacustrine, glacial (G) and glaciolacustrine (GL) sediments. Also shown are the Paudeze (PF) and Lutrive (LF) faults separating the Plateau Molasse, Molasse à charbon (MC) and Molasse rouge (MR). The close-up inset shows MTD A, the underlying deformed basin-plain units and the distal unit interpreted as a slide-evolved mass-flow deposit. The location of the line is indicated in Fig. 1. Water depth calculated for an acoustic velocity of 1500 m/s.

and regional pollen zones (Ammann, 1989; Ammann et al., 1996; Gaillard, 1984).

3.4. Numerical modelling

We investigated the potential of a subaqueous mass movement of the observed volume for generating a tsunami on the lake using numerical modelling. Simulations were carried out by numerically solving the shallow water equations in two dimensions (Simpson and Castellort, 2006). Model parameters such as deposited volume, position of failure scar, and extent of the deposit were constrained from seismic data. The velocity of the mass movement, here identified as a slide, was calculated using the equation from Ward and Day (2002). A more detailed description of parameters used can be found in Supplementary Appendix B (Supplementary Methods).

4. Results and interpretation

4.1. The 'Grand Lac' record

4.1.1. General setting

Several distinct seismic facies are present in the studied interval. A lower unit, well imaged on airgun and watergun data, has gently dipping, high-amplitude continuous reflections with sharp lateral truncations (Fig. 2). This unit, already described in previous seismic reflection studies ('Molasse' in Dupuy, 2006; 'Unit U0' in Fiore et al., 2011), is interpreted as Molasse bedrock (Plateau Molasse, Molasse à charbon, Molasse rouge) eroded by glacial activity, as known from drillings in the 'Petit Lac' (Moscariello et al., 1998) and numerous onshore studies (Sommaruga et al., 2012). In many areas, it is covered by a unit showing chaotic, low- to medium-amplitude reflections, interpreted as glacial–glaciolacustrine deposits.

These lower units are overlapped by a major 'infilling' unit with horizontal, laterally continuous, high-amplitude reflections and intercalated bodies with transparent to chaotic facies. This unit has an overall ponding geometry with large thickness in the basin and

drapes the underlying morphology on the lateral slopes, where it is only thin. These facies are interpreted as lacustrine deposits, with the layered facies representing hemipelagic and small-scale (centimetre sized) turbiditic background sedimentation and the intercalated transparent-chaotic bodies representing large-scale (decimetre to metre sized) mass transport deposits (MTDs).

These large-scale MTDs appear in all seismic reflection datasets, but due to the low theoretical vertical resolution, airgun data only image the very thick (metre sized) mass deposits (i.e. 'Turbidite of 563 AD', MTD A and an older MTD X, Fig. 2). The higher-resolution pinger data reveals additional MTDs (drawn with black lines in Fig. 3). The most recent MTD, which covers the entire deep Lake Geneva basin, has a volume of 0.25 km³ and originates from a major collapse of the Rhone delta in AD 563 ('Turbidite of 563 AD'; Kremer et al., 2012).

4.1.2. Large mass transport deposit offshore Lausanne (MTD A)

In this study, we focus on one specific seismic horizon (bold line in Fig. 3), which involves three individual MTDs (MTDs A to C; Figs. 2 and 3). MTD A is also the oldest MTD that could be reached with our coring system (core Ku-IV; Fig. 3a). It is located at the foot of the northern lateral slope of the 'Grand Lac', south of the city of Lausanne (Fig. 1), and it covers an area of 25 km². As inferred from seismic reflection data, the possible failure scar is situated on the lateral slope and shows escarpments reaching maximum heights of 20 m and extending laterally over more than 5 km at >100 m water depth, on a slope with an inclination of 5–6° (Fig. A2). This assumption is supported by the multibeam data, which show multiple escarpments on the northern slope of the 'Grand Lac' at water depths between 80 and 220 m along a 10 km portion of the slope, with individual segments reaching lengths of several kilometres (Figs. 4 and A2). The multiple failure scars might result from different events but as MTD A is the only very large MTD originating from the northern slope, imaged in the seismic data, we can attribute these scars to one large slope failure with a complex, segmented failure surface. Collapsed slopes, which have lost most of their sediment drape, show enhanced topographic lineaments, oriented parallel to the basin

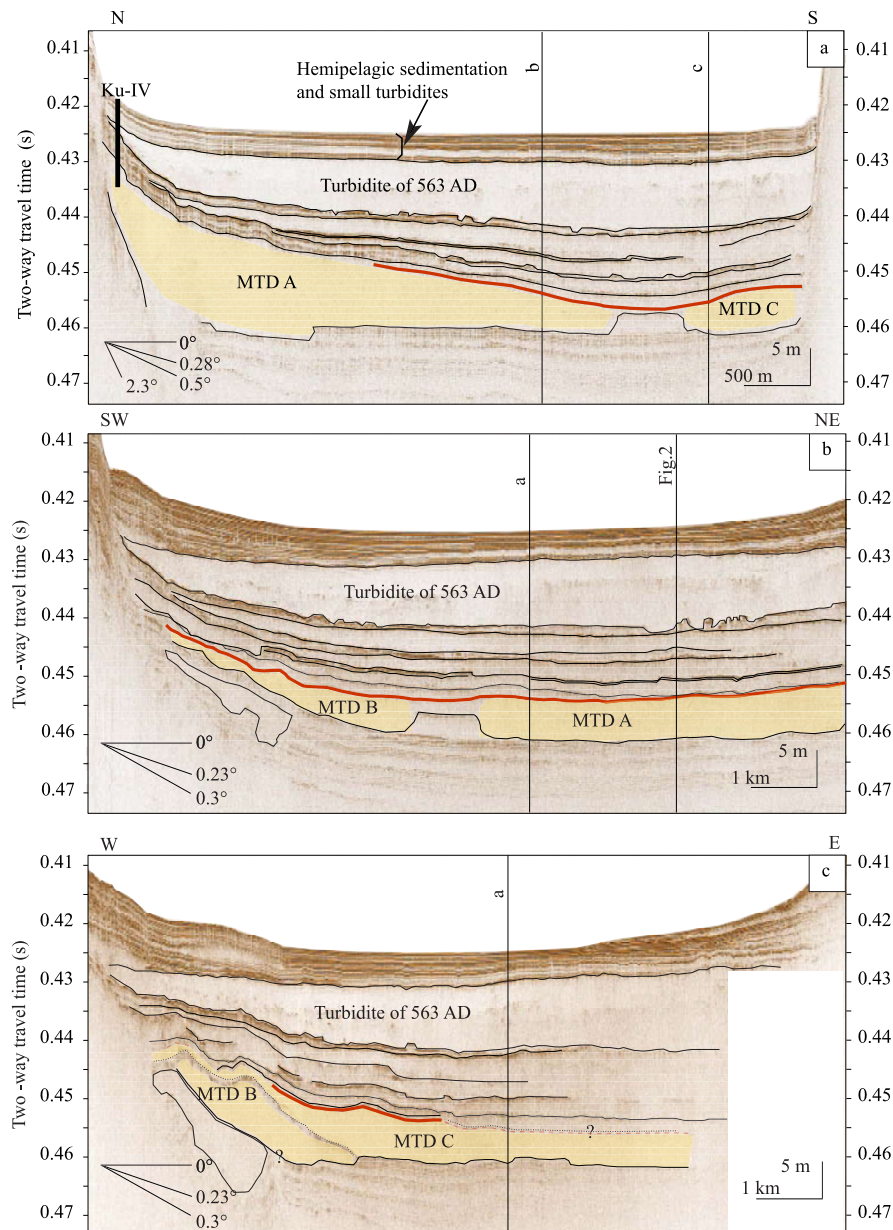


Fig. 3. Pinger seismic reflection profiles showing the relative positions of MTDs A, B and C. Bold line shows the common top horizon of the three MTDs. Position of sediment core Ku-IV is indicated in section a. The locations of these profiles are indicated in Fig. 1. Water depth was calculated for an acoustic velocity of 1500 m/s.

axis, which are interpreted as traces of the Rhone glacier advance (white dashed lines, Fig. 4) during LGM, imprinted onto underlying Molasse bedrock and compacted moraines (Dupuy, 2006). On slopes that have not failed (western and eastern ends; Fig. 4), these structures are less visible, as they are covered by a 5 to 20 m thick sediment drape. Multibeam data reveal also unusual “canyon” incisions perpendicular to the lake slope (Fig. 4). As there is no major river and/or delta nearby, these features, being distributed within the Paudeze–Lutrive fault system, suggest a possibly active tectonic zone.

On closer inspection, MTD A is characterised by two slightly differing seismic facies in the airgun data (Fig. 2). The main part is acoustically semi-transparent with some low-amplitude continuous reflections and is interpreted as a slide-evolved mass-flow (Schnellmann et al., 2006), that is frontally emergent (Moernaut and De Batist, 2011). The seismic facies at the base of MTD A is chaotic to semi-transparent with some higher-amplitude reflections and inferred faults. It is interpreted as deformed basin-plain

sediments dissected into thrust slices in response to the emplacement of the mass-flow deposit (Schnellmann et al., 2006). On the basis of the watergun and pinger seismic data, the volume of MTD A is estimated to be 0.13 km³. Seismic profiles and thickness maps show that MTD A has a maximum thickness of 20 m, with two depocentres (A1 and A2; Fig. A3).

4.1.3. Minor mass transport deposits in southern ‘Grand Lac’ basin (MTDs B and C)

On the same seismic horizon (top horizon) as MTD A, two additional MTDs B and C are identified on the basis of the high-resolution pinger data (Fig. 3a and b). MTD C appears to have been deposited shortly after MTD B (Fig. 3c). MTDs B and C are smaller in size than MTD A and cover areas of ca. 2 and 10 km², respectively, at the foot of the southern slope. These MTDs are characterised by semi-transparent seismic facies, in the pinger data, similar to MTD A. The volumes of MTDs B and C are 0.008 and 0.022 km³, respectively. The thickness map (Fig. A3)

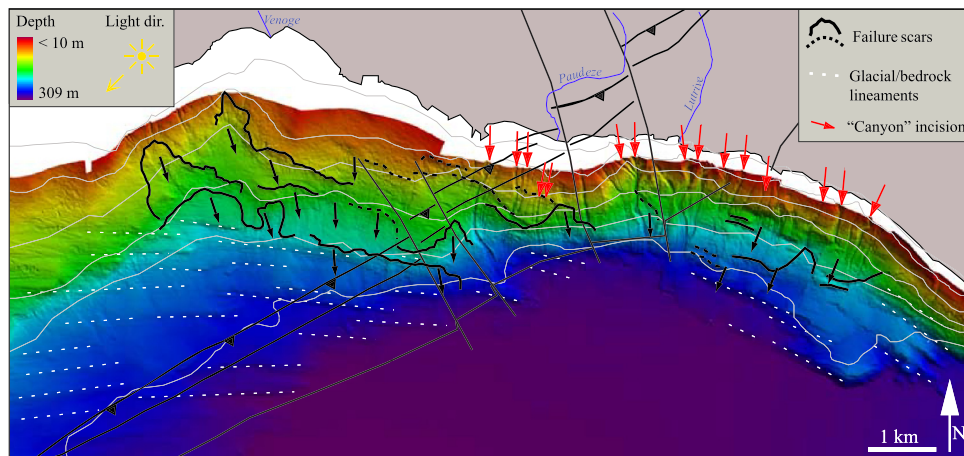


Fig. 4. Bathymetric (Direction générale de l'environnement, State of Vaud) and tectonic map (shaded relief, colour indicating depth) of the northern 'Grand Lac' slope near Lausanne reveals multiple more or less well defined failure scars from 80 to 220 m depth (black lines). Numerous "canyon" incisions, unusual outside large deltas, are interpreted as the possible surface expression of the Paudeze–Lutrive fault zone (for tectonic zone legend refer to Fig. 1). Longitudinal topographic lineaments (white dashed lines) are interpreted as traces of Rhone glacier advance (Dupuy, 2006) imprinted onto underlying Molasse bedrock and compacted moraines. The position of multibeam survey area is shown in Fig. 1.

suggests that MTD B most likely originates from the Dranse delta area, whereas MTD C possibly originates from the south-eastern lateral slope, east of the Dranse delta. Multiple mass transport deposits bounded by the same seismic top horizon are considered to be deposited simultaneously (Schnellmann et al., 2006; Strasser and Anselmetti, 2008), thus we interpret MTDs A and B as being deposited in response to the same geological event and MTD C shortly (tens of years) after MTD B as consequence of MTDs A and B, or due to another geological hazard that followed the MTD A (and B) event in a short time interval.

4.1.4. Sedimentary facies and age of MTD A

MTD A was sampled at the base of sediment core Ku-IV (Figs. 3a, 5 and A4). Ku-IV is in general characterised by silty to muddy, grey sediments interrupted by some mm- to m-scale turbidites. The base of Ku-IV, that constitutes the top of MTD A reveals a succession of ~2 m of deformed and folded laminated mud layers, followed by ~0.5 m of centimetre-scale mudclasts incorporated in a muddy matrix covered by a 0.1 m-thick layer of homogeneous, darker, faintly laminated mud with a thin, fine-grained white layer on top (Figs. 5 and A4). The lithological data, confirming the seismic interpretation, indicates that MTD A was deposited as a slide-evolved mass-flow and was topped by a homogeneous layer formed by settling of suspended fine particles after the event (Siegenthaler et al., 1987). The sediment age model for MTD A gives an interval of 1865–1608 BC (3395 ± 35 ^{14}C BP; Figs. 5 and 8, Table 1) for the homogeneous layer, revealing that MTD A happened during Early Bronze Age.

4.2. Mass transport deposit in western Lake Geneva (MTD U12)

The 70.7 m-long sediment core S3 was retrieved in the central part of the 'Petit Lac' basin at 40 m water depth (Fig. 1). It consists of a glaciolacustrine to lacustrine sediments, interrupted by a ca. 10 m-thick (6.80 to 16.60 m sediment depth) disturbed interval (U12; Fig. 6). This disturbed unit is characterised by a mixture of sand layers with near-shore material such as broken or entire gastropod shells, terrestrial vegetation remains and gravel-sized chalk pieces embedded in clayey silty lacustrine sediments (Fig. 6). The occurrence of this mixture of near-shore components and disturbed layers far from any major river input is most easily explained by a mass movement.

Palynological data confirm this sedimentological interpretation, as U12 shows two interbedded different and atypical pollen spectra (Fig. 6). The first pollen spectrum (points in Fig. 6), from 16.60 to 8.95 m and from 7.40 to 7.20 m, consists mainly of *Pinus*, *Betula*, *Artemisia*, *Poaceae* and *Chenopodiaceae*, and of mesothermophilous taxa such as *Quercus*, *Tilia*, *Ulmus* and *Fraxinus* in traces. This atypical assemblage has features of the Oldest Dryas biozone and/or Late Glacial biozone from the Swiss Plateau (Ammann et al., 2012). The second pollen spectrum (rectangles in Fig. 6), from 840 to 780 cm and at 685 cm, consists of mesothermophilous taxa such as *Quercus* and of traces of *Tilia*, *Fraxinus* and *Ulmus*, combined with *Pinus*, *Betula* and NAP taxa, which can be interpreted as an undefined Holocene biozone. Thus, in core S3, U12 is characterised by sediments containing Oldest Dryas and/or Late Glacial pollen spectra resting on top of deposits containing Holocene pollen assemblages (Fig. 6). The fact that the older biozone is very well identified below U12 and that U12 reveals a mixture of different unusual biozones, supports our sedimentological interpretation as an MTD.

A radiocarbon date from a piece of wood, sampled at 6.80 m sediment depth in a sand layer with near-shore material such as broken or entire gastropod shells, terrestrial vegetation remains and gravel-sized chalk pieces, (Fig. 6, Table 1) gives a maximum age of 1872–1622 BC (3415 ± 35 ^{14}C BP) for U12 in the 'Petit Lac'. This interval corresponds exactly to the age of MTD A in the 'Grand Lac' ± 7 years (Table 1). The mixture of sand, shells and vegetation rests suggests that the piece of wood originates from a near coastal location, thus it might have been washed and transported from on-shore into the 'Petit Lac'. However, the piece of wood might also originate from wood older than the MTD. Thus, the MTD U12 can be also much younger (some hundreds of years) than the interval 1872–1622 BC (3415 ± 35 ^{14}C BP).

4.3. Tsunami wave height simulation

In order to evaluate the consequences of a slide event related to the formation of MTD A over the lake and its shores, a simulation of a tsunami wave was carried out. Results show that the subaqueous slide has a considerable impact on the water surface of the lake, with waves reaching the directly adjacent coasts in a few minutes (Fig. 7). The first and highest waves are registered at the southern and northern lateral slope, affecting areas near Lausanne and Evian: maximum wave heights of 4 and 6 m are calculated

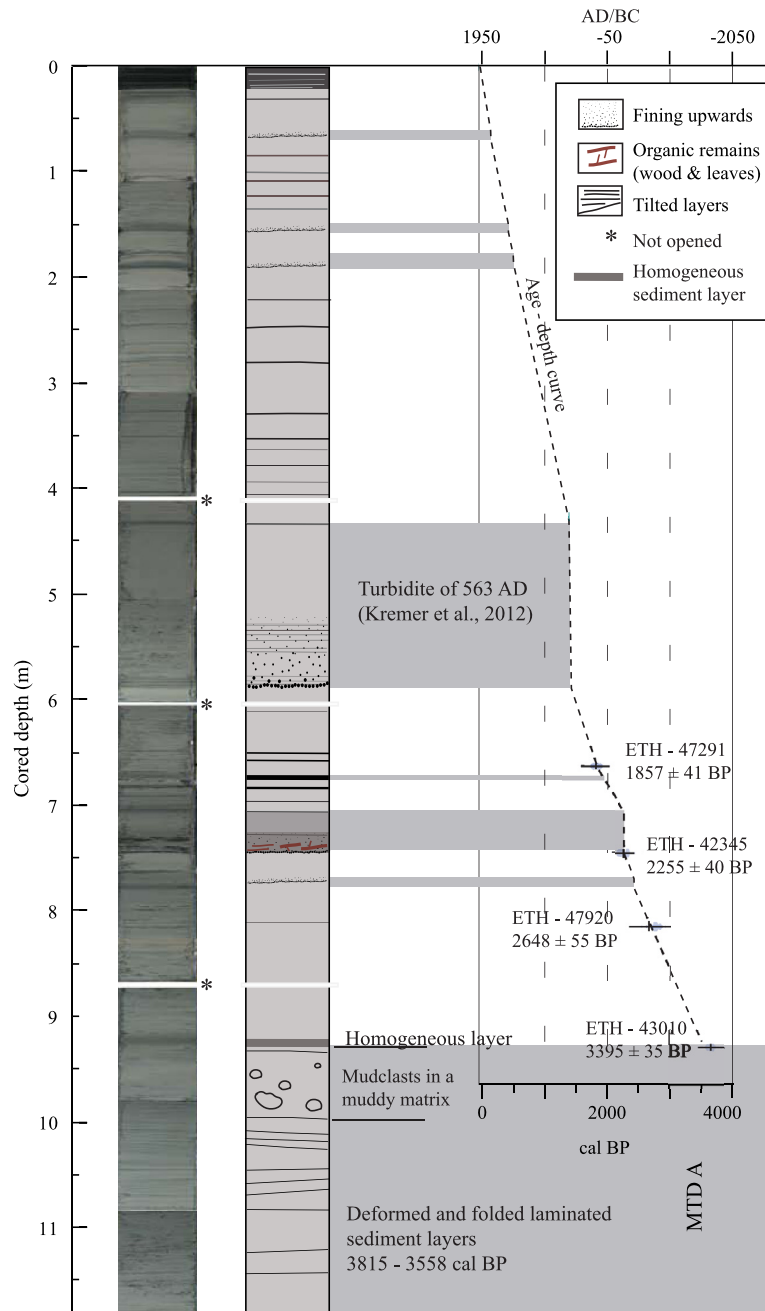


Fig. 5. Photographs and lithology of Ku-IV sediment core with turbidite and mass transport deposits outlined in grey. MTD A is composed of deformed and folded laminated sediment layers, topped by mudclasts incorporated in a muddy matrix and a homogeneous layer (images of these facies in Fig. A4). The dashed black line indicates the age–depth curve in calibrated years BP and in AD/BC as calculated by the clam script for R software (Blauw, 2010) on the basis on four ^{14}C dates (with laboratory numbers; Table 1).

3 and 6 min after slope failure at the southern (Evian) and northern (Lausanne) lateral slope, respectively (Fig. A5). In Geneva, wave heights of 1 to 2 m arrive 30 min after the slide event. Thus, the simulation shows that wave heights become smaller with distance from the slide location (Fig. A5). In most parts of the lake, the first wave is followed by a number of waves higher than the first one which are then followed by smaller (decimetre- to metre-scale) waves (Fig. A5). The tsunami might have evolved into a seiche, as it has been observed after the 1822 earthquake in Lake Bourget (Chapron et al., 1999), but we have no data to test this scenario. At the archaeological sites of Preverenges (Figs. 1 and 7), the first arriving wave of 0.75 m is relatively small, but it is followed by two waves of 1.7–1.8 m height within 15 min.

5. Discussion

5.1. Trigger mechanism

Multiple MTDs have been shown to be common geological signatures of strong historical earthquakes in subaqueous environments in the literature (Locat et al., 2003; Moernaut et al., 2007, 2009; Monecke et al., 2004, 2006; Schnellmann et al., 2002, 2006). Here we will discuss the different possible trigger mechanisms and event succession scenarios for the MTDs studied in this paper

5.1.1. Trigger mechanism of MTDs A, B and C

The location of the failure scar of MTD A at more than 80 m water depth is a strong indicator that wind waves or slow lake-

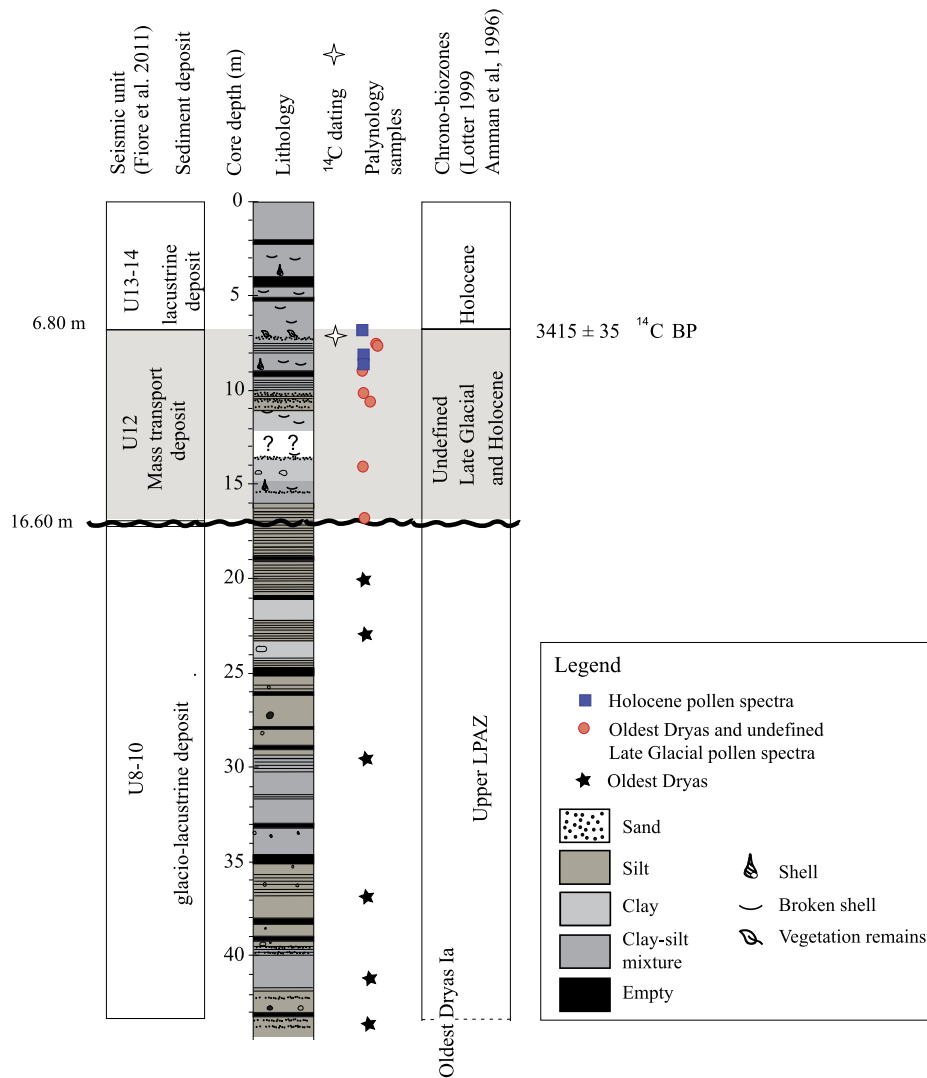


Fig. 6. Lithology of drilled sediment core S3 from the 'Petit Lac' at 40 m water depth (Fig. 1). Unit U12 is characterised by a mix of sand layers, pebbles, entire and broken shells and vegetal remains interbedded with silty – clayey lacustrine sediment, interpreted as an MTD. Palynology data of U12 show samples containing undefined Holocene pollen spectra (rectangles) embedded in unusual Oldest Dryas and undefined Late Glacial pollen spectra (points), pointing to an MTD between 1872 and 1622 BC, constrained by radiocarbon dates of leaf remains (3415 ± 35 ^{14}C BP; Table 1).

level changes (of around 2 to 3 m at that period; Corboud, 2012) can be excluded as trigger for such a failure (Schnellmann et al., 2006). Slope overloading and oversteepening are also considered of minor importance due to low sedimentation rates during the Holocene on the affected slopes, which do not receive significant sediment input from nearby rivers (<0.2 cm/yr; Thevenon et al., 2011). Therefore, considering the depth of the failure scar, the most probable trigger mechanism for MTD A is an earthquake.

For MTDs B and C, the failure scars are not imaged in seismic reflection data, and therefore the effects of wind waves and lake-level changes have to be taken into account as possible trigger mechanisms. For MTD B, with an inferred source area near the Dranse river delta (Fig. 1), oversteepening and overloading are also possible triggers. Although the exact sequence of MTDs A, B and C in the deep basin of Lake Geneva cannot be definitively resolved, these deposits from the same seismic-stratigraphic horizon seem to have been deposited in a very short interval. As shown in the numerical simulation, the mass movement responsible for MTD A may have induced tsunami waves of up to +4 m/–2 m on the southern lake shores. Tsunami waves are able to trigger secondary mass movements due to rapid erosion on the lake shores as well as rapid lake-level changes (Schnellmann et al., 2006). Thus,

it is possible that the instabilities leading to MTDs B and C were triggered by the tsunami related to MTD A, even if they are not directly linked to the main shock of a strong earthquake or to its aftershocks. However as the sequence of the MTDs cannot be completely solved, we have to keep in mind that the cause the MTDs may not be linked to each other. However this option would suggest that in short time interval (tens of years) the slopes of the deep Lake Geneva basin are collapsing during different geological events, where at least MTD A is certainly caused by an earthquake.

5.1.2. Trigger mechanism of MTD U12

The origin of the MTD recorded in the 'Petit Lac' cannot be determined with certainty. Slopes at this location in the 'Petit Lac' are gentle ($\sim 2^\circ$) and water depth is shallow (40 m), so various trigger mechanisms are possible. However, there is no river delta nearby and the almost perfect overlap in ^{14}C age is a strong indication of a possible link between MTD A in the 'Grand Lac' and the MTD U12 in the 'Petit Lac'. This implies that MTDs A and U12 were deposited coevally between 1872 and 1608 BC (Fig. 8). Results of the numerical wave height simulation of the tsunami generated by MTD A suggest a ~ 1 m wave in the 'Petit Lac'. Such a wave height is similar to those generate by strong winds (Bruschin and

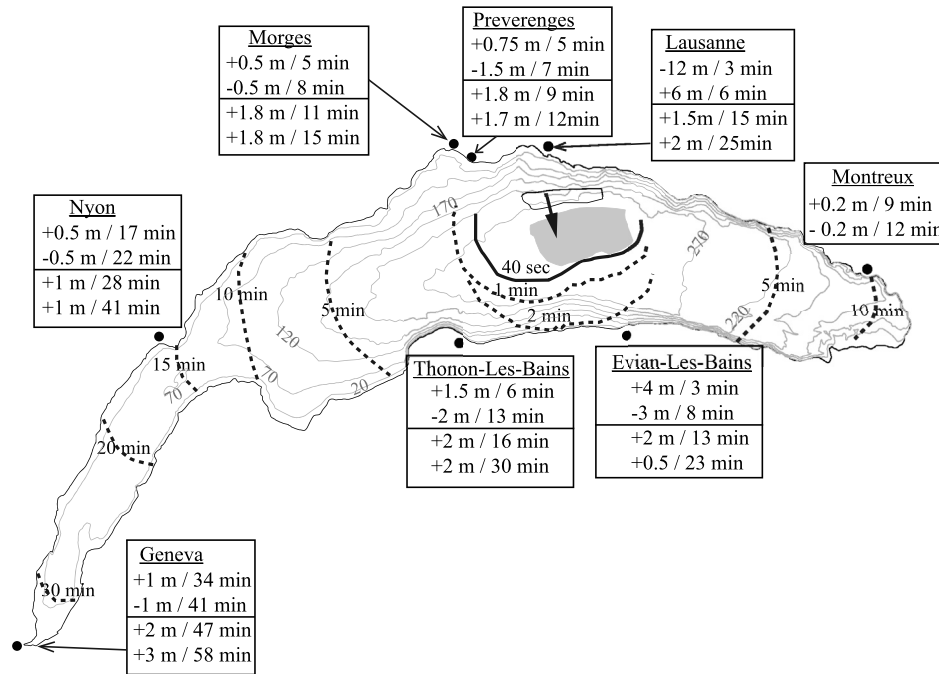


Fig. 7. Simulated tsunami wave propagation after a subaqueous slide of 0.13 km^3 (MTD A) from a scar (black contour lines) on the northern lake slope with its depocentre shown in grey. The black arrow indicates the propagation direction. Wave fronts are shown with black lines and the corresponding time in minutes. For each city shown on the map the tsunami wave heights and their corresponding arrival time are indicated. The upper part of the box reveals the first maximum and minimum wave height while the lower part of the box shows the two following maximum wave heights, resulting from waves reflected from the shore.

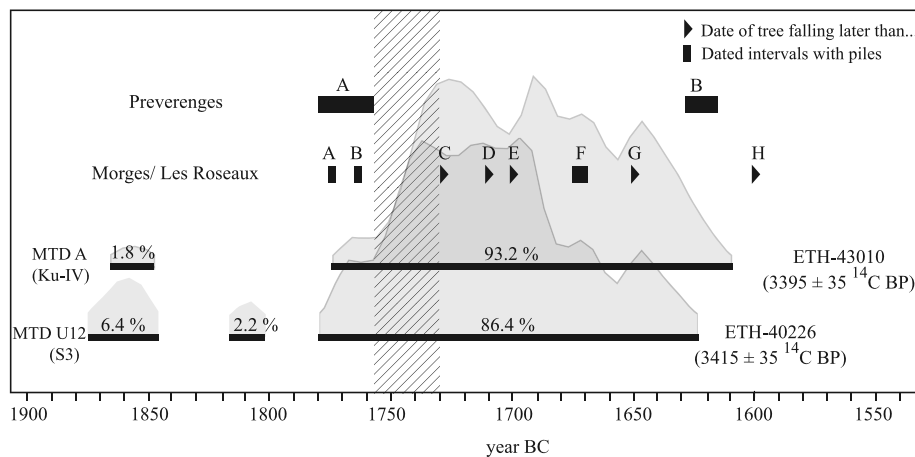


Fig. 8. Lake dwellers occupation periods of palafitte sites (located in Fig. 1; Corboud and Pugin, 2008; Corboud, 2012) from dendrochronology compared to radiocarbon dated MTDs from drilled sediments S3 (ETH-40226; Table 1) and sediment core Ku-IV (ETH-43010; Table 1), with 95% confidence intervals (calibrated distribution of the dates in grey). The dashed area indicates the inferred 28 years occupation gap of the palafitte sites.

Schneiter, 1978) and therefore we consider it as an unlikely trigger mechanism for MTD U12 in the 'Petit Lac'. Consequently, a common strong earthquake for MTDs A and MTD U12 could be taken into account as a possible trigger mechanism. However, as the absolute age of MTD U12 is based on a single piece of wood, we may consider that MTD U12 is younger than MTD A. This would mean that two different earthquakes could have separately triggered MTD A in the 'Grand Lac' and MTD U12 in the 'Petit Lac' within this interval of 150 years.

In summary, seismic reflection, sedimentological and palynological data along with ^{14}C ages all point to several major subaqueous mass movements likely caused by an earthquake during Early Bronze Age. Combining radiocarbon dates from MTDs A and U12, the multiple mass movements happened in Lake Geneva be-

tween 1872 and 1608 BC. We consider two possible scenarios to explain our observations if the MTDs are linked to each other: (1) the earthquake triggered all mass movements that lead to the deposits MTDs A to C and U12, generating a tsunami on the lake, or (2) the earthquake triggered two major mass movements (MTDs A and U12), which generated a tsunami leading to two additional failures (MTDs B and C) on the southern lateral slope of the lake in a second phase. If we consider the MTDs to not have occurred during the same geological event, then the MTDs might be explained (1) by at least two earthquakes to have generated MTDs A to C at one time and MTD U12 later or (2) all MTDs are not linked to each other and are triggered by different geological events and thus, at least two earthquakes at different times (within 150 to some hundreds of years time interval) were responsible for MTDs A and U12.

5.2. Regional seismicity

Previous studies determined minimum intensities of VII required for causing large-scale subaqueous slope failures in peri-Alpine lakes (Monecke et al., 2004). The seismicity in the Lausanne region, from historical and instrumental data (Fäh et al., 2011), points to an active Paudeze–Lutrive fault system. However, recorded earthquakes with epicentres in this region only reached maximum magnitudes Mw 2–4 and maximum intensities of V–VI (Fig. A1, Table A1), which is below the threshold value for triggering of large-scale failures and certainly excluding the observed coeval mass transport deposits (MTDs A and U12) at 40 km distance. However, historical and instrumental seismicity record covers a relatively short period of time in comparison with the age of the MTDs considered here. Strong earthquakes along the Paudeze and Lutrive Faults at earlier periods of time cannot be excluded.

Major historical earthquakes in Lake Geneva region occurred in the prealpine and alpine area. Moderate to strong earthquakes (Mw 5.5 to 6.2) happened during historical time in the western Alps 70 km east of the lake (in the Rhone valley, Wallis, Switzerland; Arnaud et al., 2002; Fritsche et al., 2012). Indeed, this area shows increased seismicity compared to the rest of Switzerland with one Mw 6 earthquake every century during the last 500 years (Fritsche et al., 2012). However reconstructed intensities of VI were too low to generate slope failure in Lake Geneva. The strongest event in the Lake Geneva region was recorded in 1584 in Aigle with reconstructed magnitude of 5.9 ('a' in Fig. A1 and Table A1; Fritsche et al., 2012). This earthquake caused a tsunami in the eastern part of Lake Geneva (Fritsche et al., 2012) and it was potentially strong enough to generate mass transport due to slope failures in the 'Grand Lac', but no major MTD has been recorded in the seismic data. An improved age model is needed in order to relate this event to one of the centimetre- to decimetre-scale turbidites that are recorded in the upper part of the sediment core. However, such a magnitude would probably not be large enough to trigger mass movement in the 'Petit Lac', where the reconstructed intensity was ~VI (Fritsche et al., 2012). Attenuation models of Bakun and Scotti (2006) of the French Alps supported this hypothesis, as for an intensity of VII an earthquake of Mw 5 is needed within 15 to 20 km epicentral distance. Taking into account a minimum VII intensity to trigger coeval slope failures in the 'Grand' and 'Petit Lac', the Early Bronze Age event of Lake Geneva could be explained by a Mw ~ 6 earthquake potentially located in the Chablais, south of the lake, where magnitudes of historical events reached already Mw 4.6–5.5 during the last 200 years ('c', 'g', 'h' in Fig. A1; Table A1; Fäh et al., 2011).

If we consider that the events in the 'Grand Lac' and 'Petit Lac' happened independently from each other, smaller earthquake magnitudes (Mw 4–5) dependent on their epicentral distance from both basins could have occurred, inferring at least 2 earthquakes within 150 to some hundreds of years. This corresponds to current frequency of light to moderate earthquakes in this region (Fritsche et al., 2012).

5.3. Early Bronze Age lake dwellers occupation gap possibly dates the catastrophic event

Irrespective of the trigger mechanism, epicentre location and the sequence of the individual MTDs, MTD A is large enough to have generated a tsunami wave on Lake Geneva in a time period that coincides with the occupation gap of the palafitte sites of Preverenges and Morges/Les Roseaux located near the major slide's failure scar. In Preverenges, where all remaining piles were dated, the occupation gap started in 1758 BC and lasted 150 years (Corboud and Pugin, 2008). In Morges/Les Roseaux, following present state of research the occupation gap ends in 1730 BC,

giving a minimum occupation at these sites of 28 years. Lake dweller's occupation gaps were previously explained by changes in lake level, soil depletion, cultural and social changes (Magny, 2004; Corboud, 2012; Magny et al., 2012; Swierczynski et al., 2013). However, available pile data from Lake Geneva's palafitte sites suggest a continuous occupation of lake dwellers between 1805 and 1600 BC (Corboud, 2012), suggesting lake levels as constant at the time of the occupation gap and, thus, very short term lake-level changes (~20 years) can be excluded. Soil depletion, cultural and social changes can explain local abandonment of settlements. High-energy events such as an earthquake followed by a tsunami are yet not taken into account as cause for the abandonment of such settlements. However, such natural hazards cannot be neglected. As the earthquake–mass movement–tsunami event coincides in time with the occupation gap of 1758 to 1730 BC at Preverenges and Morges/Les Roseaux, we propose a causal relationship between both events. Thus, archaeological data allow us to date the catastrophic chain of events that led to the lake dwellers occupation gap starting in 1758 BC (Fig. 8) in Preverenges. An earthquake followed by tsunami waves between 1 and 2 m high could have destroyed the wooden pile houses, causing death and injury in the population. This may have scared people in such a way that they abandoned the settlements during more than one generation (28 years). However, more pile data and studies on the palafitte sites and on MTDs in other lakes on the Swiss Plateau are needed to discuss a more regional cause for the occupation gap, either a more regional earthquake or a short climatic excursion.

6. Conclusion

Seismic and coring data reveal that multiple subaqueous mass movement events occurred in Lake Geneva that deposited large MTDs during Early Bronze Age. They were possibly triggered by a strong earthquake and are dated between 1872 and 1608 BC. Numerical simulation shows that the largest mass movement originating from the northern submerged slope near the city of Lausanne was large enough to create a tsunami wave of several metres along the adjacent lake shores. Dating of the MTDs and the occupation periods of two palafitte sites shows that a causal link between the MTDs and the gap of human occupation along the shores of Lake Geneva is possible. Assuming that this causal link exists, the deposition of MTDs, as well as the earthquake that is supposed to have caused them, can be precisely dated at the beginning of the human occupation gap at 1758 BC.

Acknowledgements

This work was funded by the Swiss National Science Foundation (grants no. 200021-121666 and R'Equip 133790), the 'Fondation Ernest et Lucie Schmidheiny' and by preliminary research supported by the 'Fondation Ernest Boninchi'. We thank Flavio Anselmetti, Fred Arlaud, Philippe Arpagaus, Ludovic Baron, Romain Bauer, Yves Cauderay, Laurent Decrouy, Robert Hofmann, Pierre Queloze, Reto Seifert, Chadia Volery for their help during seismic reflection and coring campaigns in the 'Grand Lac', as well as, Jehanne Correia-Demand and Ludovic Baron for their help with data processing. Thanks to Anh Dao Le Thi for providing digital coordinates for the Lake Geneva numerical model and to Adrian Gilli for access to the Limnogeology Laboratory at ETH Zurich. We particularly thank Yves Houriet, De Cérenville Géotechnique and the State of Geneva for access to the 'Petit lac' drillings of the 'Traverse du lac', as well as Katja Petrini and Chadia Volery for their help in sampling. We also warmly thank Philippe Arpagaus for perfect multibeam surveys and the 'Direction générale de l'environnement/State of Vaud' for multibeam data courtesy. We thank Chloé Pretet for helpful comments of a preliminary version of the

manuscript. We thank also Marc De Batist, Graham Kent and one anonymous reviewer for their constructive reviews.

Appendix A. Supplementary material

Supplementary material related to this article can be found online at <http://dx.doi.org/10.1016/j.epsl.2013.09.017>.

References

- Ammann, B., 1989. Late-Quaternary Palynology at Lobsigensee: Regional Vegetation History and Local Lake Development. *Dissertationes Botanicae*, vol. 137. Gebrüder Borntraeger Verlagbuchhandlung, Berlin.
- Ammann, B., Gaillard, M.-J., Lotter, A.F., 1996. In: Berglund, B.E., Birks, H.J.B., Ralska-Jasiewiczowa, M., Wright, H.E.E. (Eds.), *Palaeoecological Events During the Last 15,000 Years: Regional Syntheses of Palaeoecological Studies of Lakes and Mires in Europe*. John Wiley & Sons Ltd., New York, pp. 659–666 (Chap. 18).
- Ammann, B., van Leeuwen, J.F.N., van der Knaap, W.O., Lischke, H., Heiri, O., Tinner, W., 2012. Vegetation responses to rapid warming and to minor climatic fluctuations during the Late-Glacial Interstadial (GI-1) at Gerzensee (Switzerland). *Palaeogeogr. Palaeoclimatol. Palaeoecol.* <http://dx.doi.org/10.1016/j.palaeo.2012.07.010>.
- Arnaud, F., Lignier, V., Revel, M., Desmet, M., Beck, C., Pourchet, M., Charlet, F., Trentesaux, A., Tribouillard, N., 2002. Flood and earthquake disturbance of ^{210}Pb geochronology (Lake Anterne, NW Alps). *Terra Nova* 14, 225–232.
- Bakun, W.H., Scotti, O., 2006. Regional intensity attenuation models for France and the estimation of magnitude and location of historical earthquakes. *Geophys. J. Int.* 164, 596–610.
- Baster, I., Girardclos, S., Pugin, A., Wildi, W., 2003. High-resolution seismic stratigraphy of a Holocene lacustrine delta in western Lake Geneva (Switzerland). *Eclogae Geol. Helv.* 96, S11–S20.
- Blaauw, M., 2010. Methods and code for 'classical' age-modelling of radiocarbon sequences. *Quat. Geochronol.* 5, 512–518.
- Bruschin, J., Schneider, L., 1978. Caractéristiques des vagues dans les lacs profonds. Vagues de bise sur le Léman (Petit-Lac), campagne de mesures 1974–1978. *Bull. Tech. Suisse Romande* 19, 1–8.
- Chapron, E., Beck, C., Pourchet, M., Deconinck, J.F., 1999. 1822 earthquake-triggered homogenite in Lake Le Bourget (NW Alps). *Terra Nova* 11, 86–92.
- Corboud, P., 2012. L'archéologie lémanique un siècle après F.A. FOREL, quelques questions encore à résoudre. *Arch. Sci.* 65, 237–248.
- Corboud, P., Pugin, C., 2008. Organisation spatiale d'un village littoral du Bronze ancien lémanique: Prévéranges I VD. *Annuaire d'Archéologie Suisse* 91, 39–58.
- Corella, J.P., Arantegui, A., Loizeau, J.-L., DelSontro, T., le Dantec, N., Stark, N., Anselmetti, F.S., Girardclos, S., in press. Sediment dynamics in the subaquatic channel of the Rhone delta (Lake Geneva, France/Switzerland). *Aquat. Sci.* <http://dx.doi.org/10.1007/s00027-013-0309-4>.
- Deichmann, N., Clinton, J., Husen, S., Edwards, B., Haslinger, F., Faeh, D., Giardini, D., Kaestli, P., Kradolfer, U., Wiemer, S., 2012. Earthquakes in Switzerland and surrounding regions during 2011. *Swiss J. Geosci.* 105, 463–476.
- Dupuy, D., 2006. Etude des sédiments quaternaires, de la Molasse et sa tectonique, dans le Grand Lac (Léman) à partir de données sismiques 2D et 3D. PhD thesis. Faculté des géosciences et de l'environnement de l'Université de Lausanne, Switzerland. 253 pp.
- Fäh, D., Giardini, D., Kästli, P., Deichmann, N., Gisler, M., Schwarz-Zanetti, G., Alvarez-Rubio, S., Sellami, S., Edwards, B., Allmann, B., Behtmann, F., Wössner, J., Gassner-Stamm, G., Fritsche, S., Eberhard, D., 2011. ECOS-09 Earthquake Catalogue of Switzerland Release 2011. Report and Data. Public catalogue, 17.04.2011.
- Fiore, J., 2007. Quaternary subglacial processes in Switzerland: Geomorphology of the Plateau and seismic stratigraphy of Western Lake Geneva. *Terre et Environnement* 69. University of Geneva, Switzerland. 184 pp.
- Fiore, J., Girardclos, S., Pugin, A., Gorin, G., Wildi, W., 2011. Würmian deglaciation of western Lake Geneva (Switzerland) based on seismic stratigraphy. *Quat. Sci. Rev.* 30, 377–393.
- Fritsche, S., Fäh, D., Schwarz-Zanetti, G., 2012. Historical intensity VIII earthquakes along the Rhone valley (Valais, Switzerland): primary and secondary effects. *Swiss J. Geosci.* 105, 1–18.
- Gaillard, M.-J., 1984. A palaeohydrological study of Krageholmssjön (Scania, South Sweden). Regional vegetation history and water-level changes. LUNDQUA Report 25, 40 pp.
- Girardclos, S., Baster, I., Wildi, W., Pugin, A., Rachoud-Schneider, A.M., 2003. Bottom-current and wind-pattern changes as indicated by Late Glacial and Holocene sediments from western Lake Geneva (Switzerland). *Eclogae Geol. Helv.* 96, S39–S48.
- Girardclos, S., Fiore, J., Rachoud-Schneider, A.M., Baster, I., Wildi, W., 2005. Petit-Lac (western Lake Geneva) environment and climate history from deglaciation to the present: a synthesis. *Boreas* 34, 417–433.
- Gorin, G.E., Signer, C., Amberger, G., 1993. Structural configuration of the western Swiss Molasse Basin as defined by reflection seismic data. *Eclogae Geol. Helv.* 86, 693–716.
- Kelts, K., Briegel, U., Ghilardi, K., Hsu, K., 1986. The limnogeology–ETH coring system. *Schweiz. Z. Hydrol.* 48, 104–115.
- Kremer, K., Simpson, G., Girardclos, S., 2012. Giant Lake Geneva tsunami in AD 563. *Nat. Geosci.* 5, 756–757.
- Locat, J., Martin, F., Locat, P., Leroueil, S., Levesque, C.L., Konrad, J.-M., Urgeles, R., Canals, M., Duchesne, M.J., 2003. Submarine mass movements in the upper Saguenay Fjord (Québec, Canada), triggered by the 1663 earthquake. In: Locat, J., Mienert, J., Boisvert, L. (Eds.), *Submarine Mass Movements and Their Consequences*. Kluwer, Dordrecht, pp. 509–519.
- Loizeau, J.-L., 1991. La sédimentation récente dans le delta du Rhône, Léman: processus et évolution. PhD thesis. Université de Genève, Switzerland. 225 pp.
- Loizeau, J.-L., Girardclos, S., Dominik, J., 2012. Taux d'accumulation de sédiments récents et bilan de la matière particulaire dans le Léman (Suisse–France). *Arch. Sci.* 65, 81–92.
- Lotter, A.F., 1999. Late-glacial and Holocene vegetation history and dynamics as shown by pollen and plant macrofossil analyses in annually laminated sediments from Soppensee, central Switzerland. *Veg. Hist. Archaeobot.* 8, 165–184.
- Magny, M., 2004. Holocene climatic variability as reflected by mid-European lake level fluctuations, and its probable impact on prehistoric settlements. *Quat. Int.* 113, 65–79.
- Magny, M., Arnaud, F., Billaud, Y., Marguet, A., 2012. Lake-level fluctuations at Lake Bourget (eastern France) around 4500–3500 cal. a BP and their palaeoclimatic and archeological implications. *J. Quat. Sci.* 27, 494–502.
- Moernaut, J., De Batist, M., 2011. Frontal emplacement and mobility of sublacustrine landslides: Results from morphometric and seismostratigraphic analysis. *Mar. Geol.* 285, 29–45.
- Moernaut, J., De Batist, M., Charlet, F., Heirman, K., Chapron, E., Pino, M., Brummer, R., Urrutia, R., 2007. Giant earthquakes in South-Central Chile revealed by Holocene mass-wasting events in Lake Puyehue. *Sediment. Geol.* 195, 239–256.
- Moernaut, J., De Batist, M., Heirman, K., Van Daele, M., Pino, M., Brummer, R., Urrutia, R., 2009. Fluidization of buried mass-wasting deposits in lake sediments and its relevance for paleoseismology: Results from a reflection seismic study of lakes Villarrica and Calafquen (South-Central Chile). *Sediment. Geol.* 213, 121–135.
- Monecke, K., Anselmetti, F.S., Becker, A., Schnellmann, M., Sturm, M., Giardini, D., 2006. Earthquake-induced deformation structures in lake deposits: A late Pleistocene to Holocene paleoseismic record for central Switzerland. *Eclogae Geol. Helv.* 99, 343–362.
- Monecke, K., Anselmetti, F.S., Becker, A., Sturm, M., Giardini, D., 2004. The record of historic earthquakes in lake sediments of Central Switzerland. *Tectonophysics* 394, 21–40.
- Moscariello, A., Pugin, A., Beck, C., Chapron, E., De Batist, M., Girardclos, S., Ochs, S.I., Rachoud-Schneider, A.-M., Signer, C., Cauwenbergh, T.V., 1998. Déglaciation würmienne dans les conditions lacustres à la terminaison orbitale du bassin lémanique (Suisse occidentale et France). *Eclogae Geol. Helv.* 91, 185–201.
- Mulder, T., Cochon, P., 1996. Classification of offshore mass movements. *J. Sediment. Res.* 66, 43–57.
- Reimer, P.J., Baillie, M.G.L., Bard, E., Bayliss, A., Beck, J.W., Blackwell, P.G., Ramsey, C.B., Buck, C.E., Burr, G.S., Edwards, R.L., Friedrich, M., Grootes, P.M., Guilderson, T.P., Hajdas, I., Heaton, T.J., Hogg, A.G., Hughen, K.A., Kaiser, K.F., Kromer, B., McCormac, F.G., Manning, S.W., Reimer, R.W., Richards, D.A., Southon, J.R., Talamo, S., Turney, C.S.M., van der Plicht, J., Weyhenmeyer, C.E., 2009. Intcal09 and Marine09 radiocarbon age calibration curves, 0–50,000 years cal BP. *Radiocarbon* 51, 1111–1150.
- Reynaud, C., 1982. Etude stratigraphique, sédimentologique et palynologique des dépôts du Pléistocène supérieur au sud du bassin genevois. PhD thesis. Université de Genève, Switzerland. 190 pp.
- Scheidt, M., Marillier, F., Thierry, P., 2005. Detailed 3D seismic imaging of a fault zone beneath Lake Geneva, Switzerland. *Basin Res.* 17, 155–169.
- Schnellmann, M., Anselmetti, F.S., Giardini, D., McKenzie, J.A., 2006. 15,000 years of mass-movement history in Lake Lucerne: Implications for seismic and tsunami hazards. *Eclogae Geol. Helv.* 99, 409–428.
- Schnellmann, M., Anselmetti, F.S., Giardini, D., McKenzie, J.A., Ward, S.N., 2002. Pre-historic earthquake history revealed by lacustrine slump deposits. *Geology* 30, 1131–1134.
- Siegenthaler, C., Finger, W., Kelts, K., Wang, S., 1987. Earthquake and seiche deposits in Lake Lucerne, Switzerland. *Eclogae Geol. Helv.* 80, 241–260.
- Simpson, G., Castellort, S., 2006. Coupled model of surface water flow, sediment transport and morphological evolution. *Comput. Geosci.* 32, 1600–1614.
- Smith, S.B., Karlin, R.E., Kent, G.M., Seitz, G.G., Driscoll, N.W., 2013. Holocene subaqueous paleoseismology of Lake Tahoe. *Geol. Soc. Am. Bull.* 125, 691–708.
- Sommer, A., Eichenberger, U., Marillier, F., 2012. Seismic Atlas of the Swiss Molasse Basin. *Mat. Geol. Suisse, Geophys.*, vol. 44. Edited by the Swiss Geophysical Commission.
- Strasser, M., Anselmetti, F.S., 2008. Mass-Movement Event Stratigraphy in Lake Zurich: A Record of Varying Seismic and Environmental Impacts. *Beiträge zur Geologie der Schweiz Geotechnische Serie*, vol. 95. Zurich, Switzerland, pp. 23–41.

- Strasser, M., Anselmetti, F.S., Fäh, D., Giardini, D., Schnellmann, M., 2006. Magnitudes and source areas of large prehistoric northern Alpine earthquakes revealed by slope failures in lakes. *Geology* 34, 1005–1008.
- Strasser, M., Monecke, K., Schnellmann, M., Anselmetti, F.S., 2013. Lake sediments as natural seismographs: A compiled record of Late Quaternary earthquakes in Central Switzerland and its implication for Alpine deformation. *Sedimentology* 60, 319–341.
- Swierczynski, T., Lauterbach, S., Dulski, P., Brauer, A., 2013. Late Neolithic Mondsee Culture in Austria: living on lakes and living with flood risk? *Clim. Past* 9, 1601–1612.
- Thevenon, F., Graham, N.D., Chiaradia, M., Arpagaus, P., Wildi, W., Pote, J., 2011. Local to regional scale industrial heavy metal pollution recorded in sediments of large freshwater lakes in central Europe (lakes Geneva and Lucerne) over the last centuries. *Sci. Total Environ.* 412, 239–247.
- Vernet, J.-P., Horn, R., Badoux, H., Scolari, G., 1974. Etude structurale du Léman par sismique réflexion continue. *Eclogae Geol. Helv.* 67, 515–529.
- Ward, S.N., Day, S., 2002. Suboceanic landslides. In: Graw-Hill, M. (Ed.), 2002 Yearbook of Science and Technology. New York, pp. 349–352.
- Weidmann, M., 1998. Feuille 1243 Lausanne. *Atlas Géologique Suisse 1:25 000 Carte et Notice expl.* 85.
- Wilhelm, B., Arnaud, F., Sabatier, P., Magand, O., Chapron, E., Courp, T., Tachikawa, K., Fanget, B., Malet, E., Pignol, C., Bard, E., Delannoy, J.J., 2013. Palaeoflood activity and climate change over the last 1400 years recorded by lake sediments in the north-west European Alps. *J. Quat. Sci.* 28, 189–199.